

**Arun Dev Sharma<sup>1</sup>**  
**Inderjeet Kaur<sup>1</sup>**

## Targeting glucose metabolism by using bioactive 1-8 cineole for treatment of SARS-CoV : insights from *in-silico* studies 2019

**Authors' addresses:**

<sup>1</sup> Post Graduate department of Biotechnology, Lyallpur Khalsa College Jalandhar, 144001, Punjab, India

**Correspondence:**

*Arun Dev Sharma*  
Post Graduate department of  
Biotechnology, Lyallpur Khalsa  
College Jalandhar, , 144001, Punjab,  
India  
Tel.: 0181-2241466  
Fax: 91-181-2241465  
e-mail: arundevsharma47@gmail.com

**Article info:**

Received: 16 May 2021

Accepted: 27 September 2021

### ABSTRACT

SARS-Cov-2, responsible for COVID-19, is caused by RNA-based coronavirus. Recently 2<sup>nd</sup> wave of COVID-19 has devastated the pandemic worldwide. Inhibitors of glycolysis pathways have been evaluated to curtail the SARS-CoV-2 infectivity and spread in the host cells, but still at an infancy stage. Due to its key role in glycolysis, in the present study hexokinase has been cited as a key target for therapeutic drug synthesis. Molecular docking and pharmacological study of 1-8 cineole bioactive from eucalyptus essential oil were designed against hexokinase enzyme. Patch-dock analysis was used for docking. Ligand Protein 2D and 3D Interactions were also studied. Drug likes and toxicity profile was also evaluated. Cancer cell line toxicity profile was also studied. Molecular docking illustrated the perfect binding of 1-8 cineole to hexokinase protein. 2D and 3D studies revealed that hexokinase enzyme exhibited hydrogen and hydrophobic interactions with 1-8 cineole. 1-8 cineole also depicted a sufficient level of cancer cell line toxicity. Drug likeliness profiles studies provided guidelines and mechanistic scope for the identification of 1-8 cineole as a potent anti-COVID 19 drug. Therefore, it was concluded that 1-8 cineole from eucalyptus essential oil poses the therapeutic potential to combat infection of SARS-CoV-19.

**Key words:** COVID-19, Eucalyptus oil, Glycolysis, Herbal Drug

### Introduction

COVID-19 is a deadly pandemic disease caused by a single-stranded RNA virus named SARS-CoV-2 (Lim et al., 2021). According to WHO, this pandemic has caused more than half a million fatalities around the world. COVID-19 disease is associated with mild to severe symptoms including tiredness, fever, dry cough, acute inflammation in the lungs, shortness of breath, respiratory failure, and death (Bojkova et al., 2020). To combat this COVID-19, the current therapeutic management is based on supportive care like the use of lopinavir, remdesivir alone, and in combination with interferon and ribavirin with limited success (Barlow et al., 2020). Some other treatments regimes such as plasma therapy and monoclonal antibodies have been evaluated but bogged down due to logistic constraints and its large-scale evaluation. Recently several vaccine candidates viz: RNA, DNA, and recombinant targeting MP<sup>ro</sup> or Spike proteins of SARS-CoV-2 are in pre-clinical or clinical trials and being evaluated for their mass production, however, their role during this second wave of COVID-19 is still a matter of debate (Amanat and Krammer 2020). Since the in-built immune system is unable to generate a sufficient level of

protection against this virus, so there is a dire need for polypharmacological agents that not only attenuate viral replication but also modulate the host immune responses to combat viral infection.

In addition to the above immunomodulatory effects, infection of SARS-CoV-2 also modulates metabolic reprogramming of host cells by up-regulating glycolysis thus facilitate viral reproduction and infection (Amanat and Krammer 2020). A recent study by Codo et al (2020) showed that high glucose increased the infectivity of the SARS-CoV-2 virus and cytokine production which indicated the highlight that why people suffering from obesity and type 2 diabetes (T2D) diabetes are more prone to SARS-CoV2 infection (Bojkova et al., 2020). Data revealed that people with uncontrolled blood glucose levels are associated with a high fatality rate. It indicates that SARS-CoV-2 pathogenesis and the regulation of host cell metabolism are intimately connected. It was observed that the virus modulates host cell metabolism for more optimal conditions like high uptake of glucose for its efficient replication and spread (Thaker et al., 2019) (Supplementary Figure 1). The sustained hyperglycemia due to increased and uncontrolled glucose metabolism may enhance SARS-CoV-2's entry and subsequent replication in individuals with T2D (Ardestani

## RESEARCH ARTICLE

and Zahra, 2021). Cudo et al (2020) demonstrated that inhibitors like 2-deoxy-D-glucose (2-DG) inhibited virus replication thus abolished the generation of “cytokine storm”. Thus, key drug molecules which act as inhibitors of glycolysis have been advocated as potential therapeutic agents for treating viral infections (Lampidis Foundation 2020). We present here our perspective on the potential use of a bioactive compound 1-8 cineole (also known as eucalyptol) as a potential treatment modality for COVID-19.

1,8 cineole, also known as Eucalyptol, is the major component (44- 90%) of eucalyptus oil from all *Eucalyptus* plants (Hendry et al., 2009). 1,8 cineole is a monoterpenoid and cyclic ether and due to this, eucalyptus oil has been empirically used as an antimicrobial agent (Zakaryan et al., 2017). We hypothesize that 1,8 cineole from Eucalyptus essential oil poses capability to mitigate SARS-CoV-2 infection. So, the objective of the present study was to evaluate the therapeutic potential of 1-8 cineole against hexokinase, a major glycolytic enzyme, to control COVID-19. Hexokinase is a first and key enzyme implicated in glycolysis that phosphorylates hexoses (six-carbon sugars), forming hexose phosphate (Mathupala et al. 2006).

## Materials and Methods

### *Modeling of Ligand*

1-8 cineole was used as a potent ligand for the Hexokinase enzyme. 3D structure of 1-8 cineole was prepared by using SMILES and converted to “pdb” by UCSF-chimera.

### *In-silico Docking*

Hexokinase crystal structure was retrieved from pdb database (PDB id: 2nzt) (<https://www.rcsb.org/>). The target enzyme was cleaned from original inhibitors, water molecules and energy minimized by using chimera software. Dock preparation is an integral process that adds missing hydrogen atoms, corrects bond lengths, and correct charges. For molecular docking of 1-8 cineole with hexokinase, the PatchDock tool was used (<https://bioinfo3d.cs.tau.ac.il/PatchDock/>). Both ligand and targets were uploaded as pdb files and the job was executed using default settings. Various docked complexes were generated and the best one was saved as pdb file. Chimera and Biovia Discovery Studio Visualizer 2020, pLIP tools were used for analyzing binding mode, 2D and 3D interactions of docked complexes (<https://projects.biote.ut-dresden.de/plip-web/plip/index>).

### *Drug-likeness and toxicity*

Lipinski's rule of five was used to calculate drug-likeness of 1-8 cineole. For this SWISSADME prediction online tool was used (<http://www.swissadme.ch/>)

<http://lmmd.ecust.edu.cn/admetssar1/predict/>). Molinspiration tool was used to predict bioactivity score (<https://www.molinspiration.com/cgibin/properties>). Bioactivity score is like this: if active if score is >0), moderately active if score is between -5.0-0.0), inactive if score is < -5.0.

### *Active sites analyses*

For active site analysis of the 3D structure of target enzyme, CASTp (The Computed Atlas of Surface Topography of proteins) web tool was used using probe radius default value of 1.4.

### *Cell line toxicity prediction*

Cytotoxic effect of calotropin was determined using CLC-Pred (Cell Line Cytotoxicity Predictor) which is a web service for in-silico prediction of chemical compounds in cancer and non-transformed cell lines based on the structural formula. CLC-Pred (<http://way2drug.com/Cell-line/>) offers a prediction of the cytotoxicity of a chemical bioactive compound to assess the significance of the compounds' inclusion in experimental screening.

## Results and Discussion

*In-silico* docking analysis revealed the interaction of 1-8 cineole with hexokinase. Different poses illustrating dock scores are exhibited in Table 1. Dock pose with maximum dock score indicated maximum binding affinity. It was observed that 1-8 cineole successfully docked in the active site of hexokinase enzyme with dock score 3094 (Figure 1). D-glucose was also docked against hexokinase-II and very interestingly it was observed that dock score was 2852, indicating that 1-8 cineole poses high affinity towards hexokinase-II enzyme as compared to free glucose (data not shown). Hexokinase-II is composed of a large C-terminal catalytic domain and a small N-terminal regulatory domain. Each domain contains a sandwiched glucose binding site (Ralph et al., 2008). From *in-silico* analysis it was found that 1-8 cineole successfully docked between N- and C-terminal domains. According to the Plip server and Biovia studio results, the interaction of 1-8 cineole in the glucose binding pocket of hexokinase-protein was mediated by both hydrophobic and hydrogen bond interactions. Hydrophobic interactions were observed via THR 331, LEU 286, TYR 588, 331 at atomic distances of 3.78, 3.76, 3.69, and 3.78 Å, respectively (Figure 1). Hydrogen bond interactions of 1-8 cineole were also observed via ASN 208, 235, LYS 173, ASP 209, GLU 260, THR 173, GLN 291. Notably, among all residues, TYR 588 amino acid of hexokinase enzyme depicted interaction both with 1-8 cineole and D-glucose, suggesting a common substrate binding site for both ligands. CAST-P tool for active site investigation exposed the presence of interacting residues in the major cavity of

## RESEARCH ARTICLE

receptor enzyme hexokinase (Table 2). The major active site pocket was with Area (SA) of 4364 and Volume (SA) of

6092. Since 1-8 cineole poses high affinity towards HK enzyme as compared to glucose and both share common

**Table 1.** Docking analysis of 1-8 cineole molecules with hexokinase protein.

| Solution No | Score | Area   | ACE     | Transformation                        |
|-------------|-------|--------|---------|---------------------------------------|
| 1           | 3094  | 333.30 | -84.12  | 0.13 -0.33 -1.94 -3.36 14.06 3.04     |
| 2           | 3052  | 330.00 | -21.84  | 0.21 -0.87 1.00 -6.64 -66.08 31.99    |
| 3           | 3008  | 345.10 | -20.11  | 0.01 0.27 0.11 -34.52 -53.34 35.52    |
| 4           | 2982  | 317.70 | -30.80  | 0.53 1.11 3.00 -35.04 11.06 -14.64    |
| 5           | 2926  | 329.50 | -122.12 | -1.34 -0.98 -1.86 -9.90 28.43 -10.23  |
| 6           | 2912  | 371.10 | 9.96    | -1.26 0.97 -1.39 -7.70 27.31 5.45     |
| 7           | 2912  | 338.80 | -32.64  | 1.27 0.66 2.61 -3.85 7.53 -2.09       |
| 8           | 2884  | 312.60 | -116.85 | -2.97 0.80 -2.56 -38.63 -52.77 40.43  |
| 9           | 2866  | 303.30 | -74.41  | -1.74 -0.21 -2.18 -43.35 -11.05 19.98 |
| 10          | 2862  | 348.10 | 9.52    | -0.91 -0.48 -2.15 -35.79 -55.71 54.50 |
| 11          | 2846  | 350.80 | -46.16  | -1.25 1.16 0.83 -37.83 -53.83 33.84   |
| 12          | 2836  | 296.20 | -87.52  | 1.61 -1.08 -0.16 -40.80 -49.31 45.22  |
| 13          | 2832  | 293.90 | -11.57  | 0.40 0.29 1.21 12.22 6.88 17.94       |
| 14          | 2796  | 289.90 | -93.63  | 1.04 0.56 0.84 -2.47 15.44 7.43       |
| 15          | 2786  | 289.00 | -22.74  | 2.73 -0.85 1.68 -55.77 -36.27 42.17   |
| 16          | 2740  | 337.30 | -58.60  | 1.35 0.03 -1.70 -41.13 -4.40 24.24    |
| 17          | 2722  | 334.50 | -116.14 | -0.79 1.35 -1.87 -41.86 -55.28 31.66  |
| 18          | 2714  | 295.90 | -70.49  | -2.15 0.97 -1.10 1.44 -24.55 30.60    |
| 19          | 2696  | 311.00 | -72.75  | -2.55 -0.09 -2.71 -1.48 6.28 -3.62    |
| 20          | 2684  | 345.60 | -19.79  | -2.03 -0.26 -2.04 -8.14 8.30 -0.35    |

| Interacting residues and length (4 Å°)               | Binding pocket residues within 4 Å° radius |  |
|--|--|--|
| <b>H-bond interactions</b>                           | <b>Hydrophobic interactions</b>            |  |
| ASP209, ASN 208,235, GLU260, THR172, LYS173, GLN 291 | LEU286, THR331, TYR 588, 331               | SER285, MET589,300,555, GLU304, THR331, LEU286, TYR588, 331, HIS556, ASN567,557, GLY284, GLU116 ARG120 |

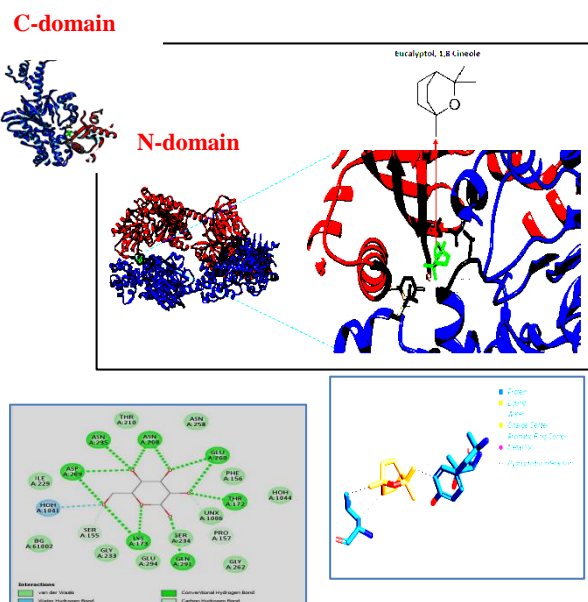


**Figure 1.** Docked complex and molecular interactions of hexokinase with 1-8 cineole

bindings site, so it absolutely was postulated that HK-protein becomes closed upon binding with 1-8 cineole that in turn induces a conformational change in HK-protein and stop further execution of glycolysis hence down-regulate the infectivity and spread of SARS-CoV-2 into the host cell. The present study results were in consonance with the earlier *in silico* findings suggesting that polypharmacological agents like 2-DG via glycolysis inhibition can act as a therapeutic for the management of COVID-19 patients (Thaker et al., 2019 ; Lampidis Foundation 2020).

Contact plot analysis showed the role of interactions between hexokinase-protein and 1-8 cineole (Figure 2). The comparison of side-chain contact plots of open (without ligand) and closed (with ligand) structures of HK-protein revealed significant conformational rearrangements upon 1-8 cineole ligand binding to HK-protein of SARS-CoV-2. This suggests the high inhibitory activity of 1-8 cineole on the HK-protein active site.

## RESEARCH ARTICLE

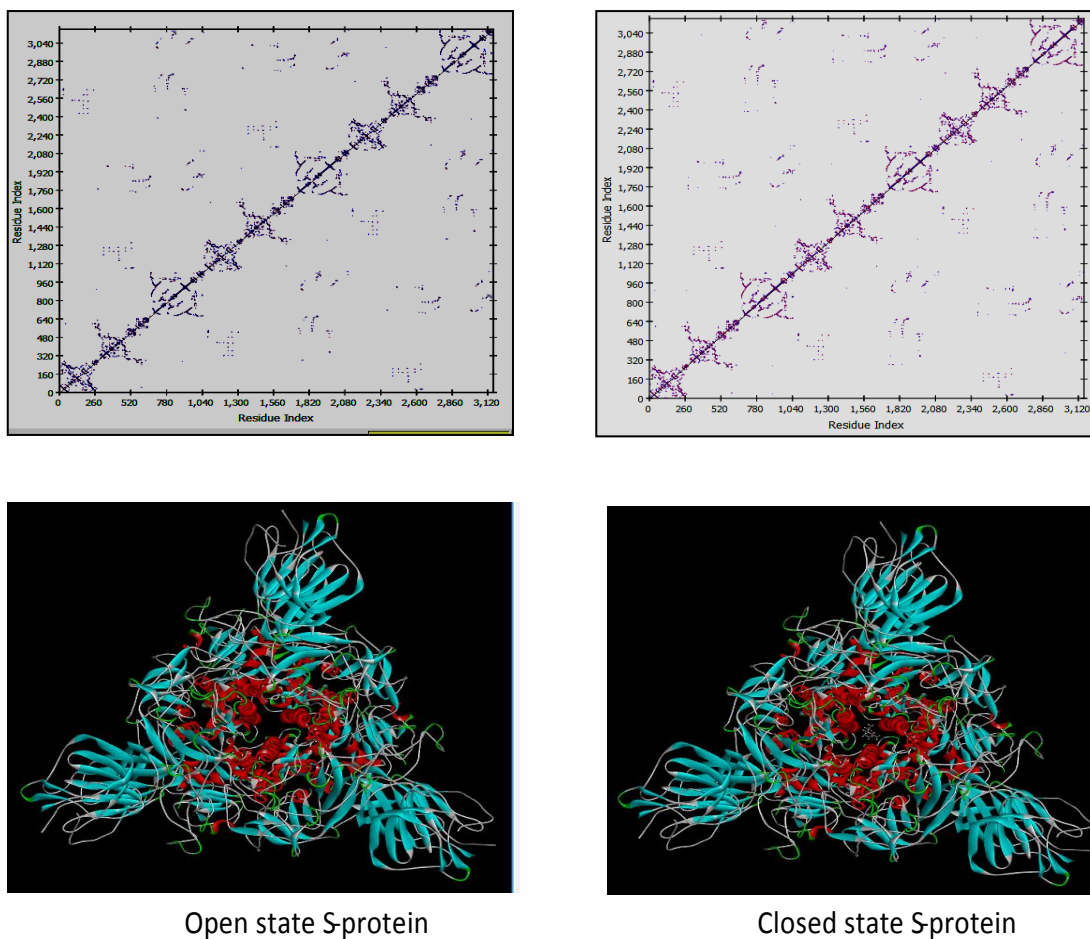


**Figure 2.** Contact plot analysis of HK-protein and HK-protein-eucalyptol complexes. Upper panel: Side chain Type plot. Arrows indicate major changes

**Table 2.** Protein target structure, native ligand and active site amino acids

| Pdb id | Macromolecule | Native ligand | Interacting Active site residues   | Cavity   |          |
|--------|---------------|---------------|--|----------|----------|
|        |               |               |  | Area     | Volume   |
| 2NZT   |               |               | THR331, LEU286, TYR588,331, ASP209, ASN 208,235, GLU260, THR172, LYS173, GLN 291 | 4364.455 | 6092.808 |

Pharmacokinetic analysis of 1-8 cineole is illustrated in Table 3. It was found that TPSA (Topological polar surface area) was  $9.23\text{ }\text{\AA}^2$ , indicating high permeability of 1-8 cineole across BBB (Blood Brain Barrier). Lipophilicity indicator as observed by Log P<sub>ow</sub> score was 2.67. Earlier studies cited that an ADMET property plays a key role in the success of any therapeutic agent in drug discovery (Wu et al., 2020). Gastrointestinal tract absorption was very high, indicating that in order to exert a toxic effect, 1-8 cineole absorbed nicely from the intestinal tract in the body. Towards Cyt -P enzymes, which are involved in toxins detoxification

84

in the liver, it was found that 1-8 cineole was non-inhibitory. MLP depicting molecular lipophilicity potential and PSA depicting a polar surface area of 1-8 cineole is shown in Figure 3. ADME properties of any drug ligand are often determined by MLP and PSA indices (for instance: membrane penetration and plasma-protein binding). Pharmacological activity describes the affirmative effects of any drug in living organisms. Drug molecules bind to biological targets such as ion channels, enzymes, and receptors. Bioactivity score of 1-8 cineole was measured for diverse parameters like binding to nuclear receptor ligand, G

**Table 3.** Pharmacokinetic analysis of EUCALYPTOL.

| Lipinski's rule of five |                       |                    |                    | ADMET properties   |               |                    |                     |              |                |                  |                                      |              |
|-------------------------|-----------------------|--------------------|--------------------|--------------------|---------------|--------------------|---------------------|--------------|----------------|------------------|--------------------------------------|--------------|
| Molecular weight        | Num. H-bond acceptors | Num. H-bond donors | Molar refractivity | lipophilicity logP | GI absorption | Consensus Log Po/w | TPSA                | BBB permeant | P-gp substrate | CYP3A4 inhibitor | Log K <sub>p</sub> (skin permeation) | Log S (ESOL) |
| 154.25 g/mol            | 1                     | 0                  | 47.12              | 2.58               | High          | 2.67               | 9.23 Å <sup>2</sup> | Yes          | No             | No               | -5.30 cm/s                           | -2.52        |

protein-coupled receptor, kinase inhibition, protease inhibition, and ion channel modulation. As shown in Table 3, bioactivity score analysis revealed that ligand 1-8 cineole was moderately active as for most of the parameters the score was

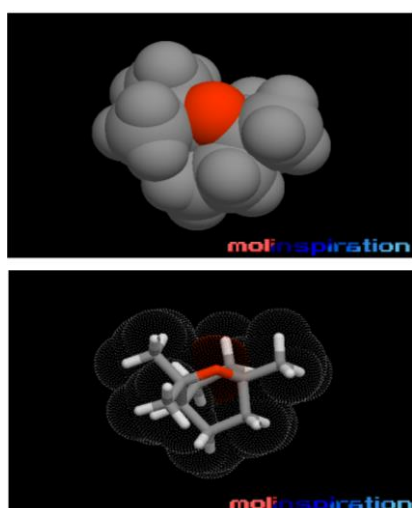
between -5.0 and 0.0.

Cell line toxicity results revealed that bioactive 1-8 cineole was toxic to tumor cell lines (Table 4). It was found

**Table 4.** Cancer cell line prediction result.

| Pa    | Pi    | Cell line                | Cell line Full name       | Tissue                             | Tumor type     |
|-------|-------|--------------------------|---------------------------|------------------------------------|----------------|
| 0.949 | 0.002 | <a href="#">NCI-H187</a> | Small cell lung carcinoma | Lung                               | Carcinoma      |
| 0.770 | 0.002 | <a href="#">Raji</a>     | B-lymphoblastic cells     | Haematopoietic and lymphoid tissue | Leukemia       |
| 0.817 | 0.003 | <a href="#">BXPC-3</a>   | Pancreatic adenocarcinoma | Pancreas                           | Adenocarcinoma |
| 0.925 | 0.003 | <a href="#">LoVo</a>     | Colon adenocarcinoma      | Colon                              | Adenocarcinoma |
| 0.908 | 0.005 | <a href="#">A549</a>     | Lung carcinoma            | Lung                               | Carcinoma      |
| 0.701 | 0.005 | <a href="#">HCT-15</a>   | Colon adenocarcinoma      | Colon                              | Adenocarcinoma |
| 0.750 | 0.005 | <a href="#">HepG2</a>    | Hepatoblastoma            | Liver                              | Hepatoblastoma |
| 0.719 | 0.007 | <a href="#">PC-3</a>     | Prostate carcinoma        | Prostate                           | Carcinoma      |
| 0.511 | 0.011 | <a href="#">A2058</a>    | Melanoma                  | Skin                               | Melanoma       |
| 0.605 | 0.032 | <a href="#">MCF7</a>     | Breast carcinoma          | Breast                             | Carcinoma      |

Pa: (probability "to be active"), Pi: (probability "to be inactive")

**Figure 3.** Molecular lipophilicity potential (MLP)/ polar surface area (PSA) views of 1-8 cineole. Hydrophobic areas: encoded by violet; Hydrophilic areas: red.

that Pa > Pi, indicated that the studied compound belonged to the sub-class of active compounds i.e. it resembles the structures of molecules, which are the most typical in a subset of "actives" in the PASS training set) as per the Way2Drug server prediction.

### Conclusion

The present findings revealed that 1-8 cineole successfully docked against Hexokinase protein. This study further suggested that 1-8 cineole has more potential to act as potential inhibitors of SARS-CoV-2. However, more *in vivo* and *in vitro* model-based studies may pave the way for these compounds in drug discovery.

### Acknowledgement

Authors want to thank management LKC for this study

### References

- Amanat F, Krammer F. 2020. SARS-CoV-2 vaccines: status report. *Immunity*. 52:583–589.

## RESEARCH ARTICLE

- Ardestani A, Zahra A. 2021. Targeting glucose metabolism for treatment of COVID-19 Signal Transduct. Target. Therapy., 6:112
- Barlow A, Landolf KM, Barlow B, Yeung SYA, Heavner JJ, Claassen CW, Heavner MS. 2020. Review of emerging pharmacotherapy for the treatment of Coronavirus Disease 2019. Pharmacotherapy. 40: 416–437.
- Bojkova D, Klann K, Koch B, Widera M, Krause D, Ciesek S, Cinatl J, M€unch C. 2020. Proteomics of SARS-CoV-2-infected host cells reveals therapy targets. Nature. 583:469–472.
- Codo A C et al. 2020. Elevated glucose levels favor SARS-CoV-2 infection and monocyte response through a HIF-1alpha/glycolysis-dependent axis. Cell Metab., 32: 437–446.
- Hendry ER, Worthington T, Conway BR, Lambert PA. 2009. Antimicrobial efficacy of eucalyptus oil and 1,8-cineole alone and in combination with chlorhexidine digluconate against microorganisms grown in planktonic and biofilm cultures. *J. Antimicro. Chemotherapy.*, 64: 1219–1225.
- Lampidis Foundation. 2020. Data supporting 2-DG as a possible treatment for COVID-19. [accessed 2021 May 10]. <http://www.lampidifoundation.org/>.
- Lim S, Bae JH, Kwon HS, Nauck M A 2021. COVID-19 and diabetes mellitus: from pathophysiology to clinical management. Nat. Rev. Endocrinol., 17: 11–30.
- Mathupala S, Ko Y, Pedersen P. 2006. Hexokinase II: Cancer's double-edged sword acting as both facilitator and gatekeeper of malignancy when bound to mitochondria. Oncogene 25: 4777–4786.
- Ralph E, Thomson J, Almaden J, Sun S. 2008. Glucose Modulation fo Glucokinase Activation by Small Molecules. Biochem., 6: 221–226.
- Thaker SK, Ch'ng J, Christofk HR. 2019. Viral hijacking of cellular metabolism. BMC Biol. ,17: 59.
- Wu C, Liu Y, Yang Y, Zhang P, Zhong W, Wang Y, Wang Q. 2020. Analysis of therapeutic targets for SARS-CoV-2 and discovery of potential drugs by computational methods. Acta Pharmaceutica Sinica B., 10: 766–788.
- Zakaryan H, Arabyan E, Oo A, Zandi K. 2017. Flavonoids: promising natural compounds against viral infections. Arch. Virol., 162: 2539–2551.